forests

MDPI

Article

Expression Patterns and Regulation of Non-Coding RNAs during Synthesis of Cellulose in *Eucalyptus grandis* Hill

Ni Zhan [1,2], Zhen Wang [3], Yaojian Xie [1], Xiuhua Shang [1], Guo Liu [1] and Zhihua Wu [1,*]

[1] China Eucalypt Research Centre, Chinese Academy of Forestry, Zhanjiang 524022, China; zhanni@gdaas.cn (N.Z.); cercxieyj@caf.ac.cn (Y.X.); cercshxh@caf.ac.cn (X.S.); cercliug@caf.ac.cn (G.L.)
[2] Institute of Fruit Tree Research, Guangdong Academy of Agricultural Sciences, Guangzhou 510640, China
[3] Beihai City Protective Forest Farm, Beihai 536000, China; wangzhen@gdaas.cn
* Correspondence: cercwzhua2889@caf.ac.cn

Abstract: Cellulose, an essential structural component in the plant cell wall and a renewable biomass resource, plays a significant role in nature. *Eucalyptus's* excellent timber tree species (including *Eucalyptus grandis* Hill) provide many raw materials for the paper and wood industries. The synthesis of cellulose is a very complex process involving multiple genes and regulated by various biological networks. However, research on regulating associated genes and non-coding RNAs during cellulose synthesis in *E. grandis* remains lacking. In this study, the wood anatomical characteristics and chemical indexes of *E. grandis* were analyzed by taking three different parts (diameter at breast height (DBH), middle and upper part of the trunk) from the main stem of *E. grandis* as raw materials. The role of non-coding RNAs (Long non-coding RNA, lncRNA; Micro RNA, miRNA; Circle RNA, circRNA) on regulating candidate genes was presented, and the network map of ceRNA (Competing endogenous RNA) regulation during wood cellulose biosynthesis of *E. grandis* was constructed. The transcriptome sequencing of nine samples obtained from the trunk of the immature xylem in *E. grandis* at DBH, middle and upper parts had a 95.81 G clean reading, 57,480 transcripts, 7365 lncRNAs, and 5180 circRNAs. Each sample had 172–306 known miRNAs and 1644–3508 new miRNAs. A total of 190 DE-lncRNAs (Differentially expressed long non-coding RNAs), 174 DE-miRNAs (Differentially expressed micro RNAs), and 270 DE-circRNAs (Differentially expressed circle RNAs) were obtained by comparing transcript expression levels. Four lncRNAs and nine miRNAs were screened out, and the ceRNA regulatory network was constructed. *LncRNA1* and *lncRNA4* regulated the genes responsible for cellulose synthesis in *E. grandis*, which were overexpressed in 84K (*Populus Alba* × *Populus glandulosa*) poplar. The cellulose and lignin content in *lncRNA4-oe* were significantly higher than wild type 84K poplar and *lncRNA1-oe*. The average plant height, middle and basal part of the stem diameter in *lncRNA4-oe* were significantly higher than the wild type. However, there was no significant difference between the growth of *lncRNA1-oe* and the wild type. Further studies are warranted to explore the molecular regulatory mechanism of cellulose biosynthesis in *Eucalyptus* species.

Keywords: cellulose; *Eucalyptus grandis*; non-coding RNA; regulatory network

Citation: Zhan, N.; Wang, Z.; Xie, Y.; Shang, X.; Liu, G.; Wu, Z. Expression Patterns and Regulation of Non-Coding RNAs during Synthesis of Cellulose in *Eucalyptus grandis* Hill. *Forests* **2021**, *12*, 1565. https://doi.org/10.3390/f12111565

Academic Editors: María-Teresa Cervera, Carmen Díaz-Sala and María Ángeles Guevara

Received: 11 October 2021
Accepted: 9 November 2021
Published: 12 November 2021

1. Introduction

Cellulose plays a vital role in plant growth and is also a renewable biomaterial [1]. The formation of cellulose is a complex biological process mediated by networks of multiple genes [2]. Competing endogenous RNA (ceRNA) are involved in complex transcriptional regulatory networks in organisms, which also includes long non-coding RNA (lncRNA), microRNA (miRNA), and circular RNA (circRNA) [3,4]. A significant portion of the eukaryotic transcriptome consists of protein non-coding RNAs (ncRNAs). Initially, these transcripts were considered transcriptional noise due to poor conservation, short half-lives, and lack of protein-coding abilities. More recently, molecular characterization of

many lncRNAs showed interaction with different types of molecules at the epigenetic, transcriptional, or translational level to modulate their targets' activities [5].

LncRNAs are RNA transcripts exceeding 200 nucleotides (nt) in length with no coding potential and are synthesized from non-functional genetic regions in eukaryotes [6]. LncRNAs act as recruiters, linkers, facilitators, traps, and signaling molecules for transcriptional, post-transcriptional, and translational regulations [7,8]. LncRNAs have been identified in *Arabidopsis thaliana* (L.) Heynh [9], rice (*Oryza sativa* L.) [10], wheat (*Triticum aestivum* L.) [11], corn (*Zea mays* L.) [12,13], cotton [14], *Selaginella moellendorffii* Hieron. [15], *Populus tomentosa* Carr. [16,17], melon [18], and *E. grandis* [19].

MiRNA is small and endogenous with a length of about 20–24 nucleotides, which regulates the gene expression process [20]. MiRNA has various regulatory roles in cells, plant organ development, and metabolic regulation and is also associated with cell proliferation, differentiation, and apoptosis [21]. MiRNAs target lncRNAs to produce phased small interfering RNAs. LncRNAs either serve as the origin or regulate the accumulation or activity of miRNAs at transcriptional and post-transcriptional levels, which is crucial for plant development, physiology, and responses to biotic and abiotic stresses [22]. Both miRNAs and lncRNAs play a significant role in cell wall biosynthesis [23]. The first miRNA was discovered in *A. thaliana* in 2002 [24]. Since then, miRNAs in rice, wheat, corn [25], *Cunninghamia lanceolate* (Lamb.) Hook., rubber (*Eucommia ulmoides* Oliv.) [26], and *Populus* spp. have also been identified.

CircRNAs are circular, closed, linear, and endogenous ncRNA molecules with a stable structure, and they regulate miRNA expression through adsorption. CircRNA could specifically bind miRNAs, inhibiting the function of regulating mRNA and regulating gene expression [27–30]. CircRNAs are widely expressed in different plants with spatiotemporal tissue-specific manifestation. CircRNA has attracted extensive attention due to its role in the growth and development of eukaryotes. Since the discovery of circRNA in the root of *A. thaliana* in 2014 [9], Andreeva and Cooper [31] reported the existence of circRNA in various animal and plant cells having many unique biological characteristics. A large number of circRNAs have been detected in rice [32], barley (*Hordeum vulgare* L.) [33], and wheat [34]. However, no analysis of ceRNAs on cellulose synthesis in *E. grandis* has been reported to date.

E. grandis is tall, straight, fast-growing, high yielding, and suitable for various growth conditions. Its wood is widely used in house building, wood-based panels, and papermaking. Moreover, it is an economic species that can meet the short-cycle demand of industrial raw material production and promote local economic development. Therefore, cellulose biosynthesis of *E. grandis* and the role of ceRNA is of great importance to understand the molecular regulation of the pathway.

In this study, immature xylem from different parts of *E. grandis* was used to establish an RNA sequencing library, and lncRNA, miRNA, and circRNA were potentially identified for their involvement in the cellulose biosynthesis pathway of *E. grandis*. To further elucidate the molecular regulation of cellulose formation in *E. grandis*, a molecular network was constructed. Two lncRNAs were cloned, their expression vectors built, and they were overexpressed in 84K poplar. This research provides a foundation for facilitating research on the molecular breeding of *E. grandis*.

2. Materials and Methods

2.1. Plant Materials and Growth Conditions

Samples of *E. grandis* were collected from a test forest in the suburb of Yibin City, Sichuan Province, China, in May 2017 (H: 375.8 m, N: 28.854098, E: 104.753013). The age of the stand was 6 years old, with a row spacing of 3.00 m × 2.00 m. In the local test forest, the air pressure was 976.0 hPa, the soil was neutral and slightly acidic, and the annual average temperature, rainfall, and sunshine were 17.90 °C, 1169.60 mm, and 1116 h, respectively. Three pieces were selected from a normally growing *E. grandis* plant with a straight trunk with no defects, diseases, or pests. About 5 mL immature xylem from different trunk

parts of *E. grandis* (Figure S1) were removed and placed in a frozen pipe filled with liquid nitrogen and later stored at −80 °C. Each sample had three biological repeats. Immature xylems at DBH (Eg-1-1, Eg-1-2, Eg-1-3), in the middle of the trunk (Eg-2-1, Eg-2-2, Eg-2-3) and at the top of the tree (Eg-3-1, Eg-3-2, Eg-3-3) were immediately collected and stored in a 2 mL cryopreservation tube. *Populus Alba* × *Populus glandulosa* (84 K poplar) was used for genetic transformation.

2.2. Measurement of Cellulose, Lignin, and Hemicellulose Content

2.2.1. Determination of Neutral Detergent Fiber (NDF) with Neutral Detergent

0.5 g sample (20–30 tons of wood powder) (W_2) was weighed and mixed with 0.5 g of anhydrous sodium sulfite, 2 mL sodium dichloride (Jinan Zhongbei Fine Chemicals Co., Ltd., Shangdong, China), and 50 mL of the neutral detergent (3% sodium dodecyl sulfate, pH = 7) (Jinan Zhongbei Fine Chemicals Co., Ltd., Shangdong, China). The reflux device was turned on, heated for 2 min to the boiling point, and kept boiling for 1 h by lowering the temperature. Then, the device was removed and kept standing for 60 s, after which it was transferred to the crucible (W_1). 300 mL distilled water at 60 °C was used for washing five times, and 30 mL acetone (Suzhou Senfeida Chemical Co., Ltd., Jiangshu, China) was used for soaking two times for 2 min. Then, acetone was used to clean, followed by extraction filtration, oven drying crucible (103 °C, 8 h), and weighing (W_3). NDF = $(W_3 - W_1)/W_2$, NDF—Neutral detergent fiber content (%), W_1: Quality of crucible (g), W_2: Dry sample quality (g), W_3: Quality of crucible and wood powder after drying (g).

2.2.2. Determination of Cellulose with Acid Detergent

1 g sample (20–30 tons of wood powder) (W_1) was weighed and heated to boiling in 100 mL of acid detergent. The reflux device was turned on, kept boiling for 60 min, and transferred to the crucible (W_2). A paste was formed by adding 72% sulfuric acid solution (Guangzhou Deli Chemical Co., Ltd., Guangdong, China) to the material in the crucible and stirred. After 3 h, 72% sulfuric acid solution was added to half of the crucible, and the temperature was kept between 20–23 °C for continuous stirring. It was followed by rinsing with hot water until neutral, drying in an oven (103 °C, 8 h), and weighing at the constant weight (W_3). Then, it was kept in a muffle furnace at 550 °C for 3 h of ashing and cooling and was finally weighed (W_4). ADF = $(W_2 - W_4)/W_1$, Cellulose = $(W_2 - W_3)/W_1$, Lignin = $(W_3 - W_4)/W_1$, Hemicellulose = NDF − ADF, ADF: Acid washing fiber content (%), W_1: Dry sample quality (g), W_2: Crucible mass (g), W3: Drying quality after acid (g), W_4: Quality of crucible and wood powder after ashing (g).

2.3. Total RNA Extraction and Detection

Total RNA was extracted according to the instructions of the TRIzol kit (Thermo Fisher Scientific, Waltham, MA, USA), and Nanodrop detected RNA concentration, 28S/18S. Then, RIN (RNA integrity number) values were detected by Agilent 2100 Bioanalyzer (Agilent Technologies, Santa Clara, CA, USA), and the quality and integrity of the extracted RNA were detected by 1% gel electrophoresis.

2.4. LncRNA Extract

After total RNA extraction, ribosomal RNA was removed with ribo-zero™ Magnetic Kit (Epicentre, Madison, WI, USA) to maximize the retention of all coding and ncRNAs. The RNA obtained was randomly broken into short fragments, then used as a template to synthesize the first strand of cDNA with random hexamers. Then buffer, dNTPs (dUTP instead of dTTP), DNA polymerase I, and RNase H were added to synthesize the second strand of cDNA. The second strand was purified by QiaQuick PCR kit (QIAGEN, Hilden, Germany), eluted with EB buffer solution, terminally repaired, base A added, and junction sequenced, then degraded by uracil-n-glycosylase (UNG) enzyme. Agarose gel electrophoresis was used for fragment size selection and PCR amplification. The Illumina

HiSeqTM 4000 platform provided by the Gene Denovo Company (Guangdong, China) was used for sequencing.

2.5. Identification and Classification of lncRNAs

Clean outputs were obtained by filtering the machine's data and were compared with the reference genome of *E. grandis* (The NCBI gcf_000612305.1) using TopHat (v2.0.10) for analysis [35]. After the reads were matched with the genome, cufflinks (v2.2.1 parameter-f0.3-j 1-a 0-p 6-library-type fr-first strand) was used for assembly generation using reference annotation-based transcript (RABT) [35]. Novel transcripts were screened on the reference genome (screening criteria: transcript length $\geq$ 200 bp, exon $\geq$ 2, plant sample $\geq$ 1) based on their location, predicted as new lncRNAs. The coding ability of the new transcript was predicted by using the Coding protein calculator (CPC) (version CPC-0.9-r2) and Coding-non-coding Index (CNCI) [36]. Meanwhile, the new transcripts were also compared to the protein database UniProt. The intersection of these transcripts without coding potential and protein annotation information was considered a reliable prediction.

2.6. Screening of Differentially Expressed lncRNAs

Cuffdiff software [35] was used to analyze the expressions of lncRNAs and genes in Eg1, Eg2, and Eg3 (FPKM value). EdgeR [37] was used to evaluate the differences in expressions of lncRNAs. False discovery rate (FDR) and log2FC (Fold change) were used for differential screening. The screening conditions were set at FDR < 0.05 and $|\log2FC| > 1$.

2.7. MiRNA Extraction and Identification Analysis

TRIzol was used to extract total RNA from the samples, followed by selecting 18–30nt fragments using agarose gel electrophoresis. Next, the 3′ and 5′ junctions were connected, and the miRNAs connected to the bilateral junctions were then subjected to reverse transcription and PCR amplification. Finally, about 140 bp strips were recovered and purified using agarose gel electrophoresis. The constructed libraries were controlled using Agilent 2100 and qPCR and sequenced by computer.

The blastall 2.2.25 (blastn) software (NCBI, Rockville, MD, USA) annotated the miRNA sequences obtained by sequencing using rRNA, scRNA, snoRNA, snRNA, and tRNA in GenBank samples and were removed as much as possible [38]. The bowtie (version 1.1.2) software was used to determine the position of the sequenced miRNA on the genome [38]. Tag sequences were used to compare the genomic location, and the mireap_v0.2 software was used to predict the unique secondary structure of miRNA and identify the new miRNA [38].

2.8. MiRNA Expression Analysis

The miRNAs identified from each sample were summarized. The expression level for each miRNA was calculated as tags per million (TPM) = $T \times 10^6/N$ (T stands for miRNA, N stands for total miRNA (existing + existing edit + known + new predicted miRNA counts)), followed by the determination of expression profiles of all miRNAs.

EdgeR software was used to analyze the differences between various miRNAs using default parameters [39]. The screening criteria for differentially expressed miRNAs were more than two times, and the *p*-value was <0.05. We also analyzed the differential expressions of all miRNAs, existing miRNAs, known miRNAs, new miRNAs, and category I miRNAs. Patmatch_v1.2 software conducted the complementary pairing of miRNA and target genes through program screening and prediction [39].

2.9. Identification of circRNAs

After extracting the sequencing data, a TopHat comparison was conducted with the reference genome to obtain the comparative results for each sample. First, the unmapped reads were extracted from the alignment results, and then both ends of each unmapped read were intercepted (default 20 bp) to get the anchors. Finally, the genome was aligned

with anchors, and the resulting alignment was submitted to Find_circ software to identify circRNAs [40].

2.10. Expression Analysis and Target Relationship Prediction of circRNAs

The expression of circRNAs was calculated using the back-spliced Reads Per Million mapped Reads (RPM) method, with RPM = 10^6 C/N. RPM (A) was the expression of gene A, C was the number of back-spliced Reads aligned to gene A, and N was the number of total back-spliced Reads aligned to the reference gene, p-value < 0.05, and $|\log2FC| > 1$, for identification of differentially expressed circRNAs. GO annotation and KEGG pathway analyses were performed for differentially expressed genes. Patmatch_v1.2 software was used to analyze all the circRNAs and the miRNAs to predict the targeted relationship [39].

2.11. RNA Reverse Transcription and q RT-PCR

Two μg of RNA was taken, and reverse transcription was performed using the Novizan reverse transcription kit (R223, QIAGEN, Hilden, Germany). Fifteen ceRNA genes were selected as validation genes and expressed in three different parts of *E. grandis* viz., trunk, leaves, and roots. The total q RT-PCR reaction system was 20 μL containing 2 X ChamQ SYBR qPCR Master Mix 10 μL, forward primer (10 μmol·L^{-1}) 0.4 μL, reverse primer (10 μmol·L^{-1}) 0.4 μL, cDNA 4 μL, and RNase Free ddH_2O 5.2 μL. The PCR amplification condition was 95 °C predenaturation for 90 s, 40 cycles of 5 s denaturation at 95 °C, 15 s of annealing at 60 °C, and 20 s of extension at 72 °C (the fluorescence signal was collected at the end of each cycle). Each analysis was repeated three times. Primers were designed by the Primer Express 2.0 Software (PE Applied Biosystems, Waltham, MA, USA) using default parameters. The primer sequences are given in Table S1. The actin gene was used as the internal reference gene, which was expressed stably during the whole growth process of *E. grandis*. The $2^{-\Delta\Delta Ct}$ method [41] and Microsoft Excel software (Albuquerque, NM, USA)were used to analyze the data.

2.12. Co-Expression of ceRNA Regulatory Network

The ceRNA co-expression regulatory network recognizes the interactions among the differentially expressed lncRNAs, miRNAs, and circRNAs. Pearson's correlations were used to calculate significant associations by constructing the co-expression network. Cytoscape 3.8.0 software was used to draw the networks [42].

2.13. Extraction of Total RNA from Immature Xylem of E. grandis and Reverse Transcription of cDNA

The immature xylem of *E. grandis* preserved at −80 °C was grounded into a finely powdered mixture with liquid nitrogen. Genomic DNA was extracted from plant powder (about 50 mg) using a tree extract-DNA reagent (Wuhan Keyue Qilin Biotechnology Co., LTD., cat. 11-02, Wuhan, China). The reverse transcription reaction was performed using the TransScript II one-step gDNA Removal and cDNA Synthesis SuperMix (Beijing Chuanjin Biotechnology Co., LTD., cat. AH311-02, Beijing, China), and the cDNA finally obtained was stored at −20 °C.

2.14. Gene Cloning and Vector Construction

Full-length sequences of XR_001980078.1 (*lncRNA1*), XR_720796.2 (*lncRNA2*), XR_727233.2 (*lncRNA3*) and XR_001985124.1 (*lncRNA4*) were obtained. Primers were designed using Primer 5.0 [43], and the sequences are shown in Table S2. PCR amplification products were cloned into pCAMBIA vectors digested by Nco1 and Pml1 through homologous recombination using the ClonExpress II One Step Cloning Kit (Nanjing Novezan Biotechnology Co., LTD., cat. C112-01/02, Nanjing, China).

2.15. Assembly of Plasmid Constructs for Plant Genetic Transformation

Positive clones were detected using colony PCR, and the plasmids were extracted and sequenced from the selected clones. The positive plasmids were transformed into *Agrobacterium* GV3101. The *Agrobacterium* colonies carrying 35S: *lncRNA1* and 35S: *lncRNA4*, respectively, were used for poplar transformation according to the protocol by Liu et al. [44] and Lu et al. [45]. In addition, positive regeneration seedlings were identified using PCR according to Etchells [46].

2.16. Positive Transgenic Plant Screening and Phenotype Analysis

Genomic DNA was isolated from transformant 84 K poplar leaves using the MiniBEST Plant Genomic DNA Extraction Kit (TaKaRa, Bao Biological Engineering (Dalian) Co., Ltd. Liaoning, China). Positive transgenic plants were identified by PCR analysis using positive test primers (Table S3). The contents of cellulose, lignin, and hemicellulose were measured from 3-week-old plants using an ELISA (enzyme-linked immunosorbent assay) kit (Qiy, Shanghai, China). Phenotype analysis for heights, root lengths, and root numbers of 84 K poplar was carried out with 3-week-old plants. In contrast, phenotype analysis for poplar heights, internode diameters, and ground diameters was carried out with 10-week-old plants. The base and the middle of the stem were observed under a microscope (LNB701C, Shanghai LNB Instrument Co., Ltd., Shanghai, China). Four independent lines were used for the phenotype analysis of the transformants in each construct. Significant differences relative to the wild-type control plants were determined by Student's *t*-test (SPSS 20.0).

3. Results

3.1. The Content of Cellulose, Lignin, and Hemicellulose

The cellulose content in *E. grandis* was significantly higher in the middle (52.9%) than in the DBH and the upper part of the trunk. Lignin content in DBH and the upper trunk was significantly higher than the middle trunk. Hemicellulose content in DBH and the middle part of the trunk were significantly higher than the upper part (Figure 1). The cellulose content differed in different trunk positions in *E. grandis*, followed by non-coding transcriptome sequencing analyses.

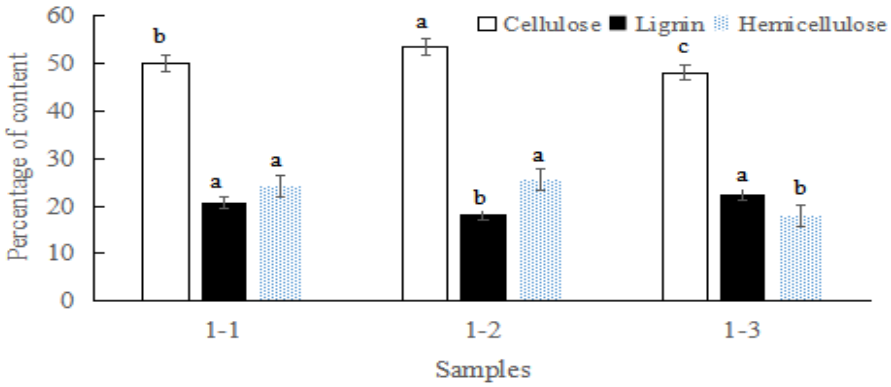

Figure 1. Contents of cellulose, lignin, and hemicellulose of *E. grandis*. 1–1 represented the DBH of the trunk. 1–2 represented the middle part of the trunk. 1–3 represented the upper part of the trunk. Different lowercase letters in the table represent significant differences at 0.05 level.

3.2. Identification and Analysis of lncRNAs in E. grandis

A large number of clean reads were obtained using high-throughput sequencing (Table S4). Reads containing rRNAs were removed, and transcriptome assembly was performed using the *E. grandis* genome as a reference. 5375 new transcripts were predicted by using the Coding protein calculator (CPC), 4464 transcripts were predicted by using the Coding-non-coding Index (CNCI) and 7694 new transcripts were compared to the protein database UniProt. Over 3445 new transcripts were found (Table S5) after removing FPKM (Fragments Per Kilobase per Million) and other low coverage sequences, and the lncRNA

prediction results from new transcripts are shown in Figure 2a. New lncRNAs can be divided into five categories based on their position relative to protein-coding genes on the genome: intergenic lncRNAs, bidirectional lncRNAs, intronic lncRNAs, antisense lncRNAs, and sense overlapping lncRNAs. In our study, the percentage of intergenic lncRNAs was the highest, and no intron lncRNA was found (Figure 2b).

The differential expression of lncRNAs was analyzed by comparing Eg-1, Eg-2, and Eg-3 (Figure 2c). It was observed that Eg-1 vs. Eg-2 identified one differentially expressed lncRNA (up-regulated). On the other hand, Eg-1 vs. Eg-3 identified 16 differentially expressed lncRNAs (six up-regulated, ten down-regulated). Likewise, six differentially expressed lncRNAs (one up-regulated, five down-regulated) were identified in Eg-2 vs. Eg-3.

3.3. Identification and Analysis of miRNA in E. grandis

Clear reads were filtered to produce clear tags (Table S6). High-throughput sequencing was performed on mir-Eg-1, mir-Eg-2, and mir-Eg-3, and the clean tags obtained are shown in Table S7. MiRNA sequences were compared to the reference genome of *E. grandis* and plant miRNAs in miRBase to identify known miRNAs, as shown in Table S8. The hairpin structure of miRNA was predicted, and the number of new miRNAs identified in each sample was counted. More than 3000 new miRNAs were detected (a maximum of 3508) in all samples except mir-Eg-2-2 (1644) (Table S9).

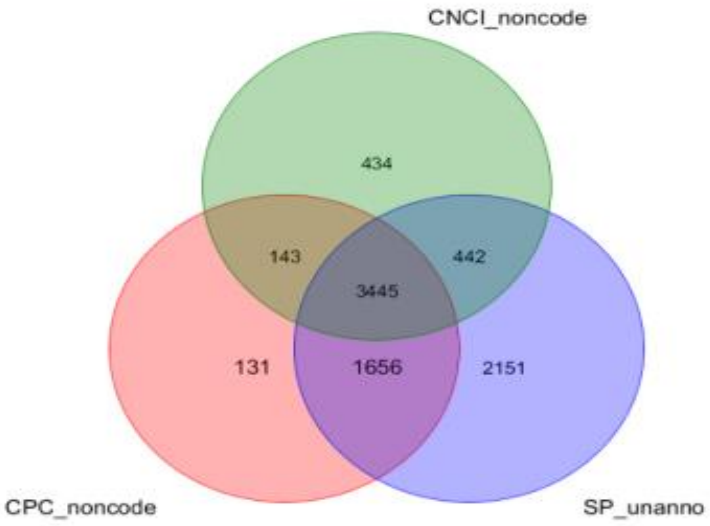

(**a**)

Figure 2. *Cont.*

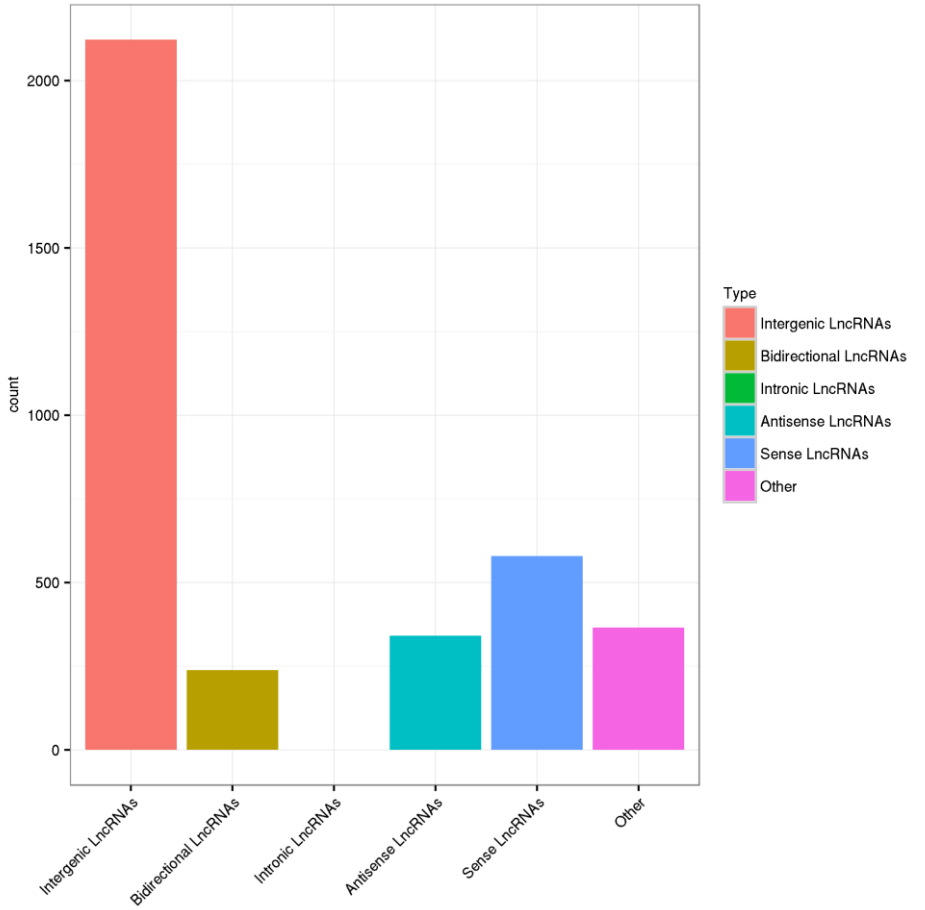

(**b**)

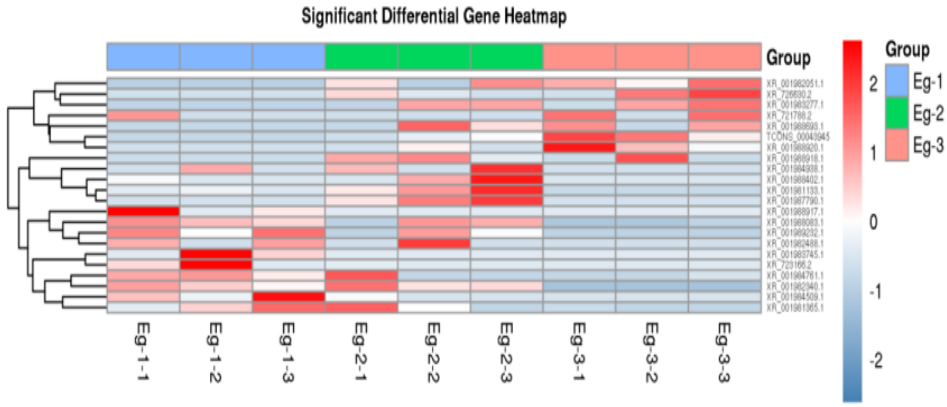

(**c**)

Figure 2. *Cont.*

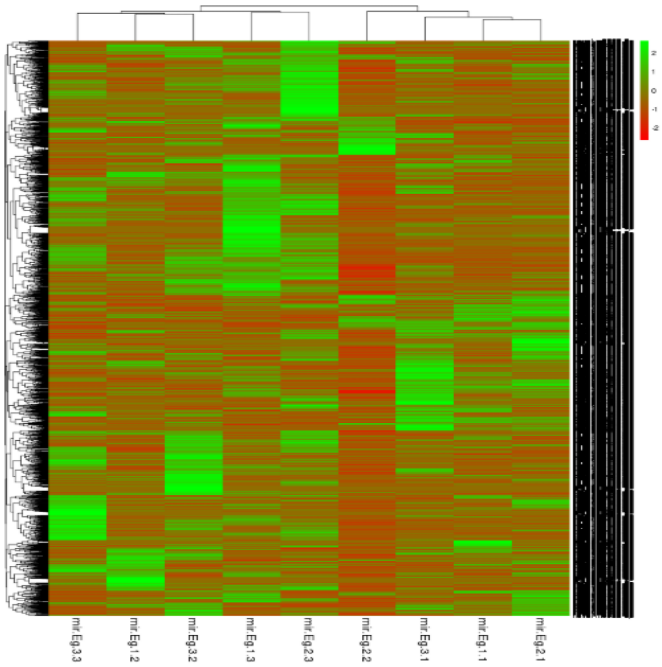

(**d**)

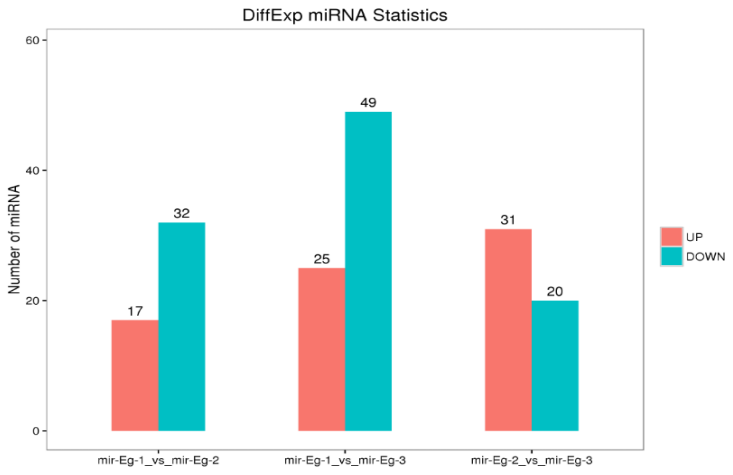

(**e**)

Figure 2. (**a**) Long non-coding RNA (lncRNAs) forecast results Venn diagram. (**b**) Statistical graph of new lncRNA transcripts. (**c**) Cluster diagram of differentially expressed lncRNA patterns between groups. (**d**) Heat map of miRNA expression. Heat maps can be clustered on two dimensions (samples, miRNA), and the topological relationship of clustering can be used to observe the relationship between samples or between miRNAs. In order to eliminate data noise, miRNAs with TPM < 1 are filtered out for heat map analysis. Based on miRNA expression, the relationship between samples and miRNA was hierarchically clustered, and the results of clustering were presented by heat map. (**e**) Statistical graph of miRNA differential expression between groups.

MiRNAs in mir-Eg-1, mir-Eg-2, and mir-Eg-3 samples showed significant differences (Figure 2d). Similarly, all miRNAs, existing miRNAs, known miRNAs, new miRNAs, and the first of a kind miRNAs were analyzed for differential expressions. Seventeen miRNAs were found to be up-regulated and 32 down-regulated in mir-Eg-1 vs. mir-Eg-2. In mir-Eg-1 vs. mir-Eg-3, 25 and 49 miRNAs exhibited up-regulation and down-regulation, respectively.

In mir-Eg-2 vs. mir-Eg-3, 31 miRNAs were up-regulated while 20 were down-regulated (Figure 2e).

The predicted number of miRNA target genes and binding sites indicate that the relationship between miRNA and target genes was one-one, one-to-many, and many-to-one (Table S10). Target genes of differentially expressed miRNAs in mir-Eg-1 vs. mir-Eg-2 samples were mainly enriched in cellular, metabolic, and single-organism processes, along with the binding and catalytic activities. Target genes of differentially expressed miRNAs in mir-Eg-1 vs. mir-Eg-3 samples were mainly associated with cellular and metabolic processes. Target genes of differentially expressed miRNAs in mir-Eg-2 vs. mir-Eg-3 samples were mainly involved in cellular and metabolic processes and binding and catalytic activities (Figure 3).

3.4. Circular RNA Statistical Analysis

CircBase database annotation was performed on circRNAs. First, annotated circRNAs were defined as existing circRNAs, while the unannotated ones were defined as new predicted circRNAs. Then, the existing circRNAs were annotated with the starBase miRNA targeting relationship and were defined as the existing targeting relationship. MiRNA targeting was predicted for all circRNAs, providing a new predictive targeting relationship. A total of 4347 miRNAs and 3871 circRNAs displayed 250,104 targeting relationships (Table S11).

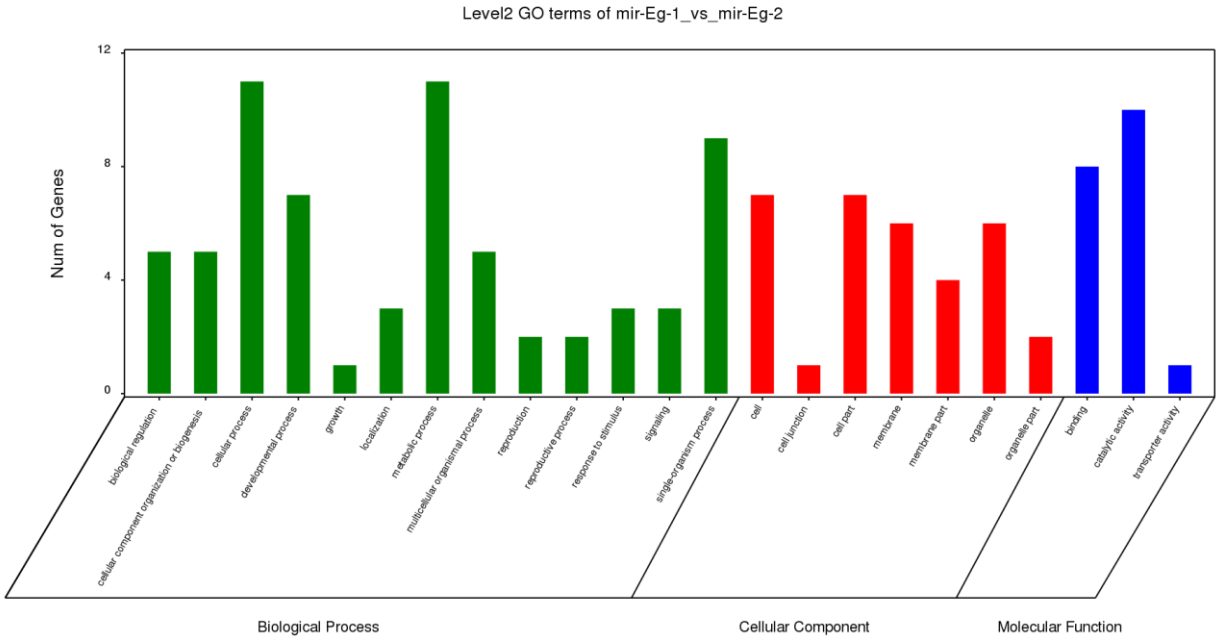

Figure 3. *Cont.*

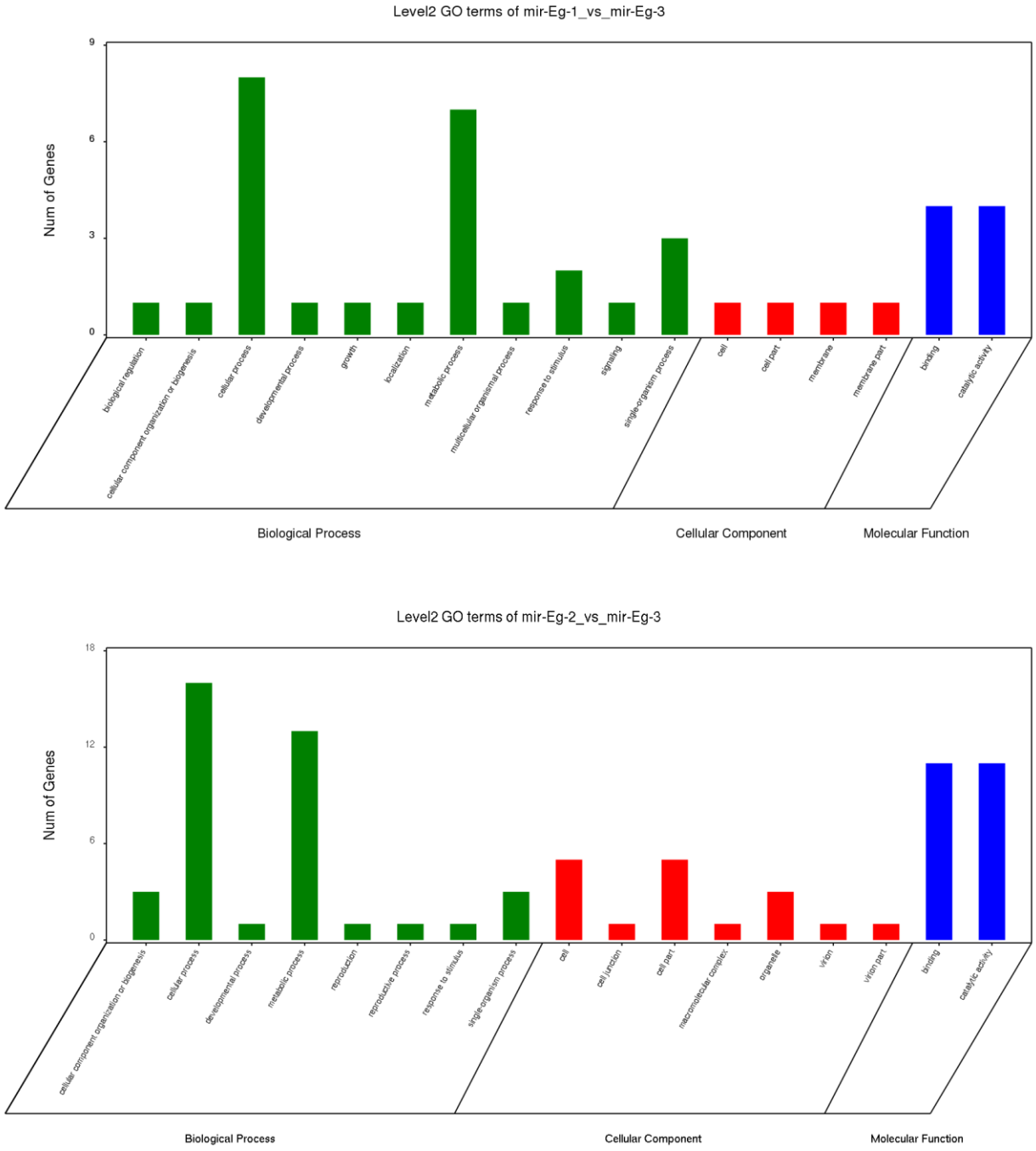

Figure 3. GO enrichment analysis of target genes in differentially expressed miRNAs between groups.

3.5. Screening of Genes Related to Cellulose Synthesis in E. grandis

Through function prediction and analysis of differentially expressed target genes, the following four lncRNAs were closely related to cellulose synthesis screened in *E. grandis*, viz., XR_001980078.1, XR_720796.2, XR_727233.2, and XR_001985124.1 (Table 1). In addition, five miRNAs closely related to cellulose synthesis were detected in *E. grandis*, which included miR5298-y, miR3951-x, miR5198-y, miR5156-x, and miR5298-y (Table 2).

Twelve non-coding RNAs were expressed in three different tissues in the trunk, leaves, and roots of *E. grandis*. The results displayed that XR_001985124.1 and XR_727233.2 were highly expressed at the top and the root of the tree. XR_720796.2 was expressed at DBH, middle, and top of the trunk but significantly in the root. Most genes were highly expressed within the roots and leaves (Figure 4). Q RT-PCR verified high throughput sequencing

results, and the expression patterns of genes were consistent with transcriptome data, depicting reliability.

Table 1. Synthesis of *Eucalyptus grandis* cellulose related lncRNAs.

Number	lncRNA	Target Gene	Symbol	Description
LncRNA1	XR_001980078.1	XM_010061899.2	RhGT1	PREDICTED: UDP-glycosyltransferase 88B1 [*Eucalyptus grandis*]
LncRNA2	XR_720796.2	XM_010030945.2	GATL9	PREDICTED: probable galacturonosyltransferase-like 9 [*Eucalyptus grandis*]
LncRNA3	XR_727233.2	XM_018877681.1	UXS6	PREDICTED: UDP-glucuronic acid decarboxylase 5 [*Eucalyptus grandis*]
LncRNA4	XR_001985124.1	XM_010048758.2	CESA7	PREDICTED: cellulose synthase A catalytic subunit 7 [UDP-forming]-like [*Eucalyptus grandis*]

Table 2. Synthesis of *Eucalyptus grandis* cellulose related miRNAs.

miRNA	Target Gene	Symbol	Description
miR5298-y	XM_018877681.1	UXS6	PREDICTED: UDP-glucuronic acid decarboxylase 5 [*Eucalyptus grandis*]
miR3951-x	XM_010030945.2	GATL9	PREDICTED: probable galacturonosyltransferase-like 9 [*Eucalyptus grandis*]
miR5198-y	NM_001302719.1	CESA5	probable cellulose synthase A catalytic subunit 5 [*Eucalyptus grandis*]
miR5156-x	XM_010055035.2	UTR4	PREDICTED: UDP-galactose/UDP-glucose transporter 2 [*Eucalyptus grandis*]
miR5298-y	XM_018877682.1	UXS6	PREDICTED: UDP-glucuronic acid decarboxylase 5 [*Eucalyptus grandis*]

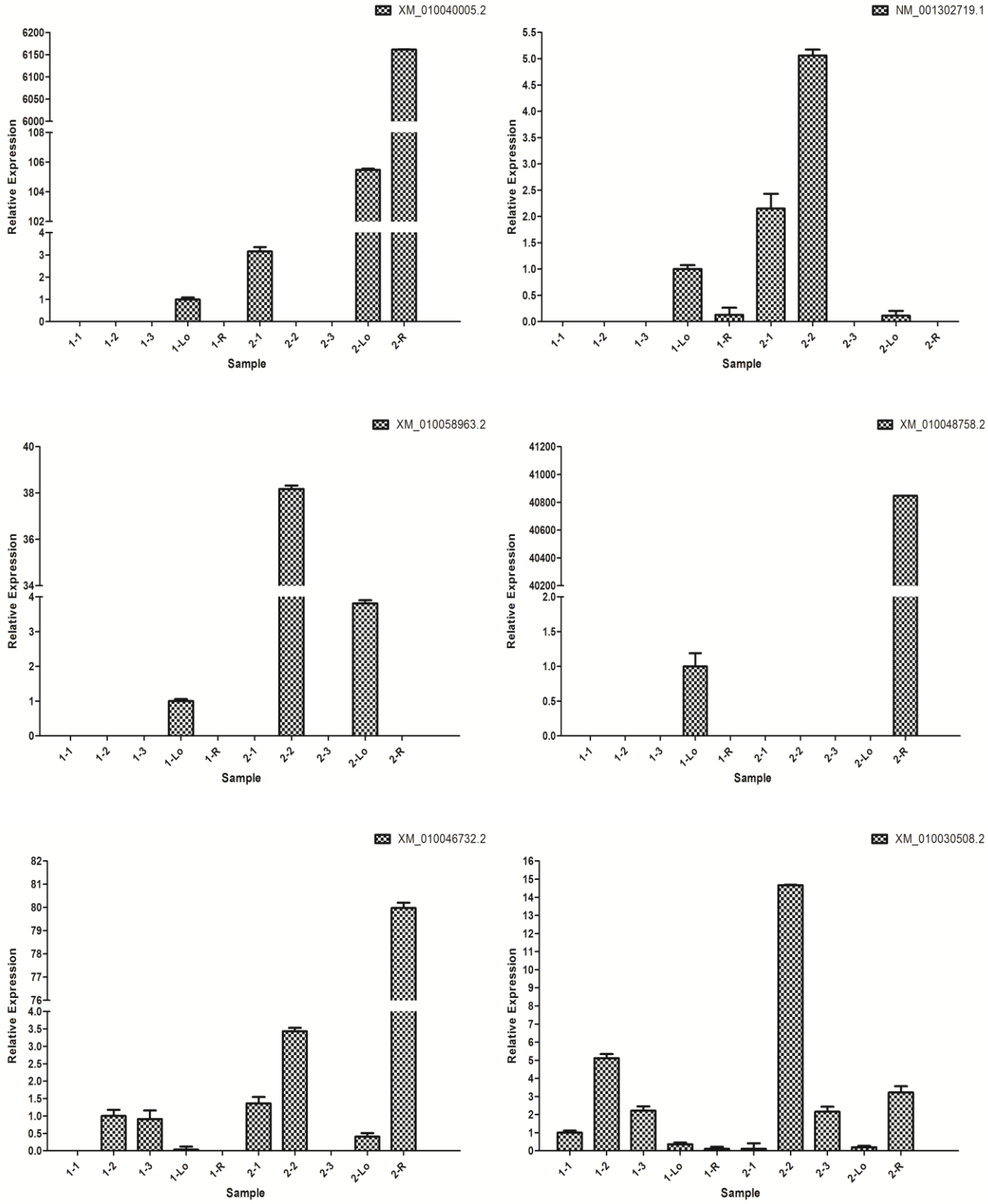

Figure 4. *Cont.*

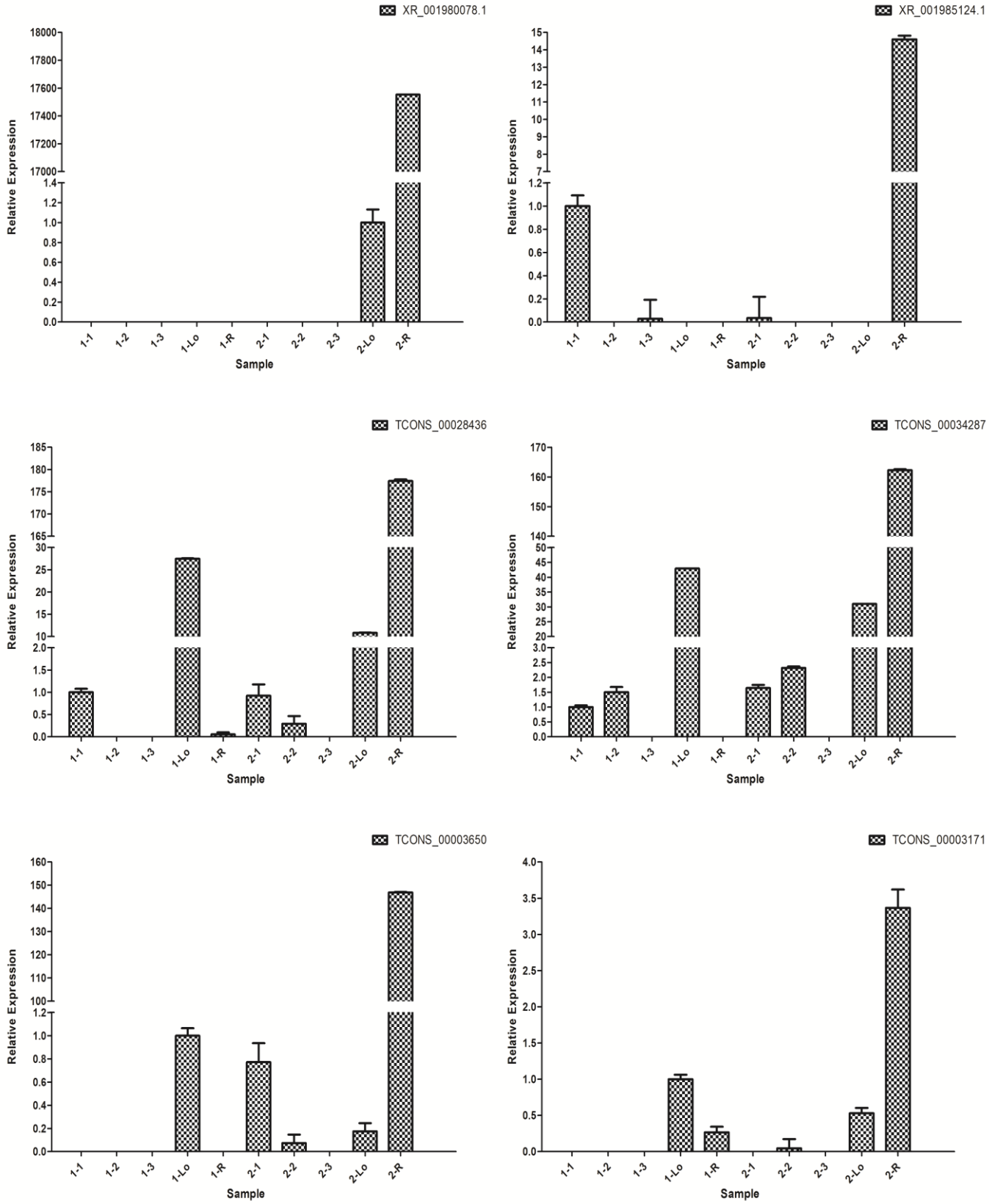

Figure 4. Results of target gene q RT-PCR. 1-1, 2-1 represented diameter at breast height of the trunk; 1-2, 2-2 represented the middle of the trunk; 1-3, 2-3 represented upper part of the trunk; 1-Lo, 2- Lo represented the leaves; and 1-R, 2-R represented the roots of *E. grandis*.

3.6. Construction of ceRNA Co-Expression Regulatory Network

Based on relatedness to cellulose synthesis, ceRNA and mRNA were screened out to construct a co-expression regulatory network, with miRNA as the center, connecting different lncRNAs, mRNAs, and circRNAs. As shown in Figure 5A, four lncRNAs, 19 mRNAs, and 17 circRNAs constituted a co-expression network with novel-m0277-5p as the center. With mir6476-x as the central node, ten lncRNAs, 18 mRNAs, and two circRNAs constituted the co-expression network (Figure 5B). A novel-m1920-3p, novel-m1950-3p, novel-m2147-5p and novel-m3931-5p constructed the central framework (Figure 5C). A novel-m1950-3p as the center, one lncRNA, one mRNA, and six circRNAs also constituted a co-expression network (Figure 5D), while another co-expression network was found with both novel-m2401-3p and novel-m4146-3p as the center (Figure 5E).

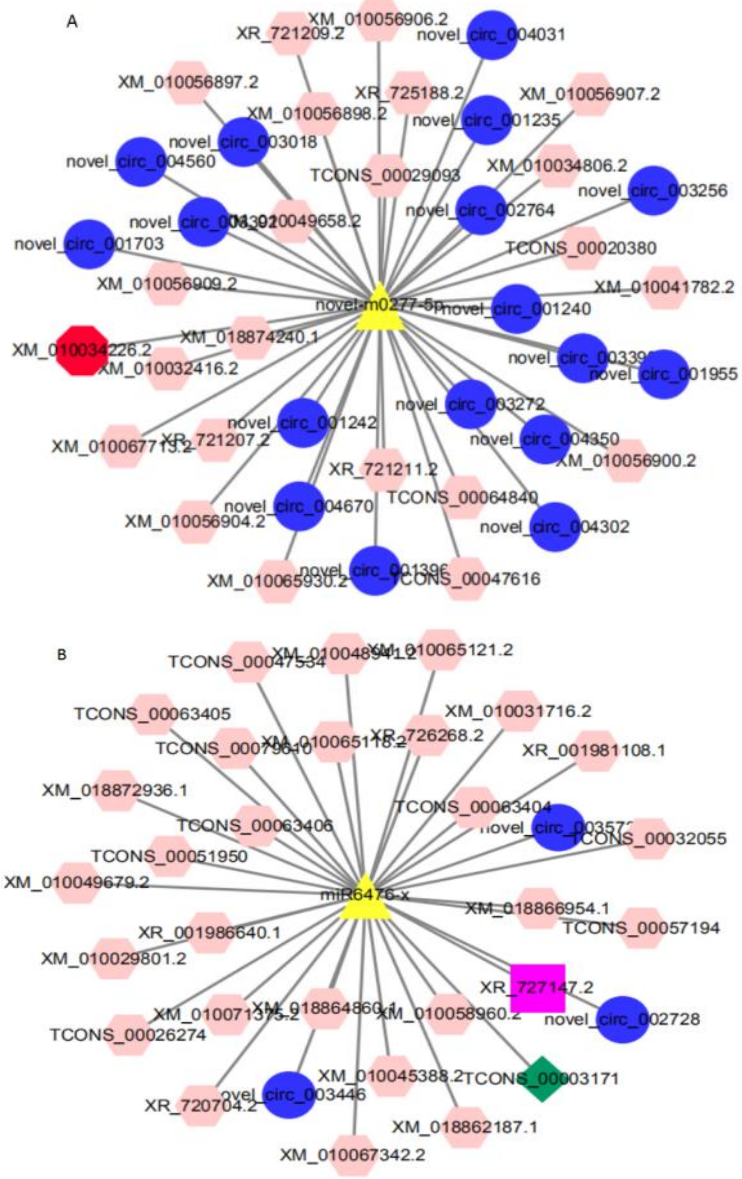

Figure 5. *Cont.*

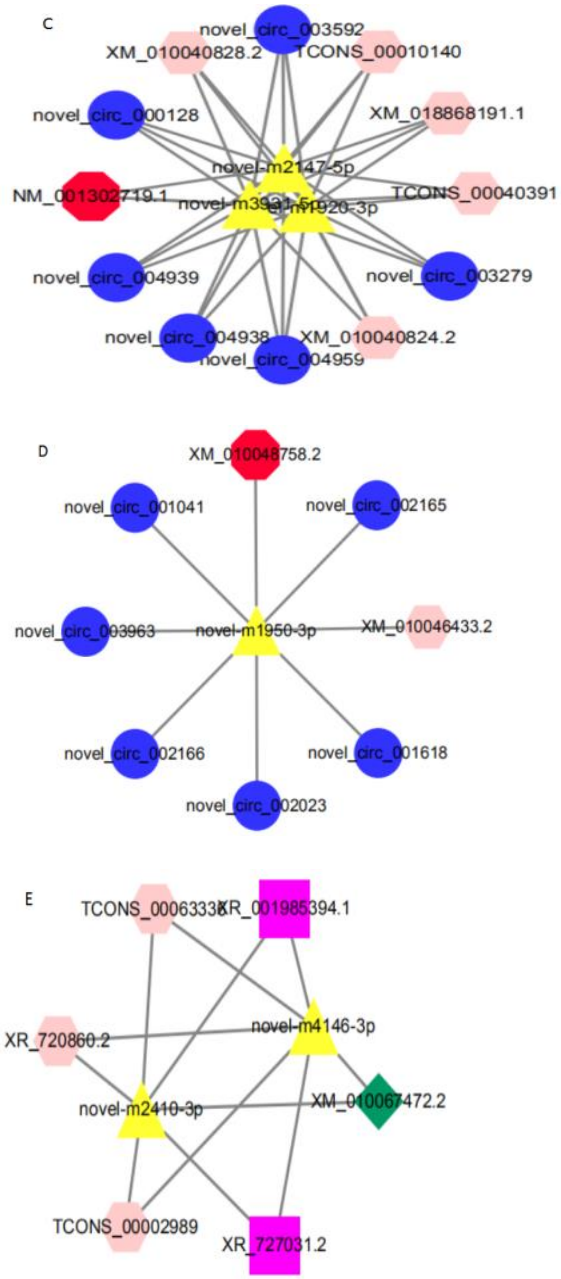

Figure 5. lncRNA-mRNA co-expression network. Pink and red hexagons represented lncRNAs and mRNAs, magenta squares represented mRNAs, green diamonds represented mRNAs, yellow triangles represented miRNAs, and blue circles represented circRNAs. (**A**), 4 lncRNAs, 19 mRNAs, and 17 circRNAs; (**B**), 10 lncRNAs, 18 mRNAs, and 2 circRNAs; (**C**), 5 lncRNAs, 1 mRNAs, and 6 circRNAs; (**D**), 1 lncRNA, 1 mRNA, and 6 circRNAs; (**E**), 3 lncRNA, 2 mRNA, and 1 circRNAs.

3.7. Gene Cloning and Vector Construction

The extracted genomic DNA is shown in Figure S2. Using a Q5 high-fidelity DNA polymerase (New England Biolabs, M0491), XR_001980078.1 (*lncRNA1*), XR_720796.2 (*lncRNA2*), XR_727233.2 (*lncRNA3*), and XR_001985124.1 (*lncRNA4*) sequences with relatedness to cellulose biosynthesis pathway were successfully amplified from the prepared genomic DNA of *E. grandis* (Figure S3). pCAMBIA vector was successfully constructed. Plasmids were then cloned from positive bacteria and identified by double enzyme digestion (Figure S4). Finally, the clones were selected for sequencing and were successfully transformed to *Agrobacterium* GV3101.

3.8. Effects of Overexpression of lncRNA1 and lncRNA4 on Plant Growth

To verify the functions of *lncRNA1* and *lncRNA4*, they were transformed into 84 K poplar, viz., *lncRNA1-oe*, and *lncRNA4-oe*, respectively (Figures S5 and S6). The results showed that cellulose, lignin, and hemicellulose contents of *lncRNA4-oe* with three-week-old plants were significantly higher than that in the *lncRNA1-oe* and wild-types (Figure 6). In addition, the average height, root lengths, and the number of roots of *lncRNA4-oe* of three-week-old plants were significantly higher than *lncRNA1-oe* and wild-types (Figure 7).

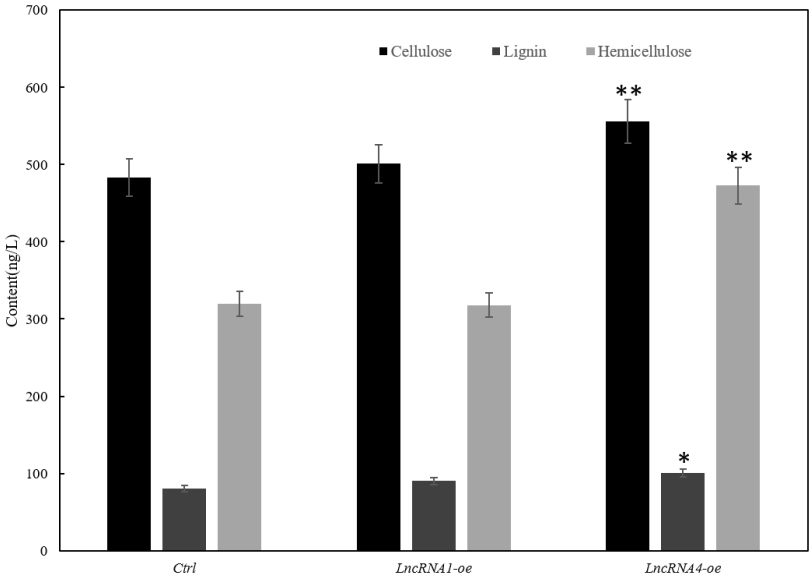

Figure 6. Component content of overexpression and wild type 84K poplar trees. Bars represented standard errors (SE), * represented the significant difference ($p < 0.05$), and ** represented the highly significant difference ($p < 0.01$). Values were reported as means ± SE ($n = 4$).

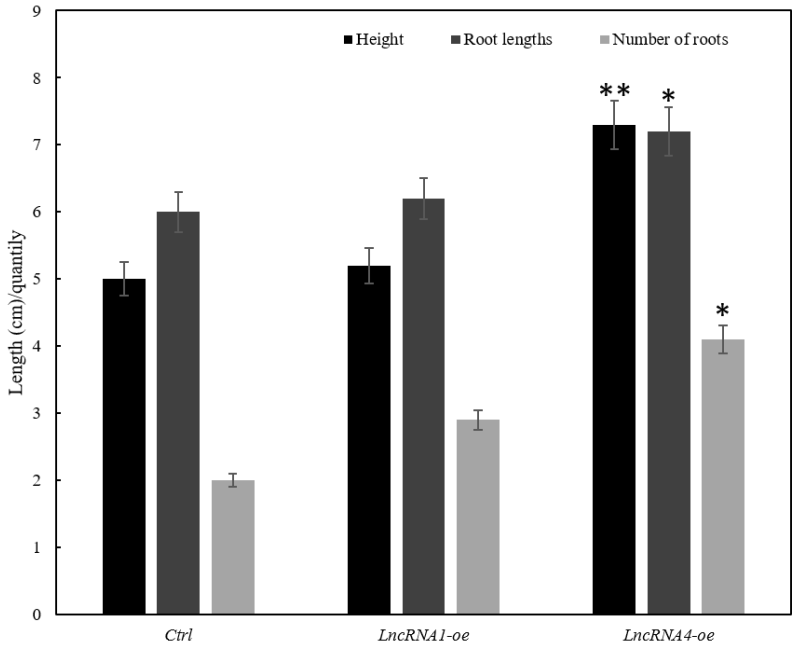

Figure 7. Plant height and root of overexpression and wild type 84K poplar trees. Bars represented standard errors (SE), * represented the significant difference ($p < 0.05$), and ** represented the highly significant difference ($p < 0.01$). Values were reported as means ± SE ($n = 4$).

The average height of *lncRNA4-oe* of ten-week-old plants was 26.31% and 22.17% higher than the controls and *lncRNA1-oe*, showing significant differences (Figure 8a). At the middle of the stem, the diameters of *lncRNA4-oe* were significantly longer than *lncRNA1-oe* and controls. At the base of the stem, the diameters of *lncRNA4-oe* were significantly longer than *lncRNA1-oe* and controls (Figure 8b). In addition, the increase of xylon cells in the middle and the base part of the *lncRNA4-oe* was significantly higher than *lncRNA1-oe* and wild type 84 K poplar (Figure 9).

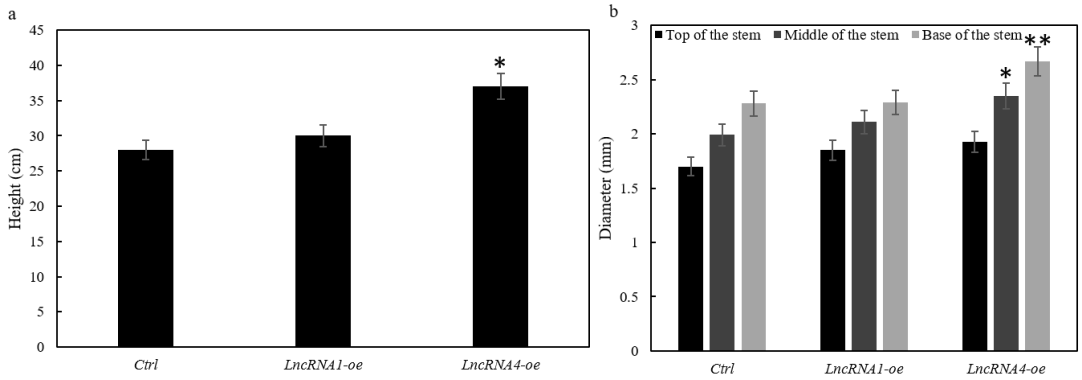

Figure 8. Statistics of plant height and internode diameter of overexpression and wild type 84K poplar trees. (**a**) represented the average plant height for ten-week-old wild type 84K, *lncRNA1-oe* and *lncRNA4-oe*. (**b**) represented the average diameter of upper, middle and basal part of stem for ten-week-old wild-type 84K, *lncRNA1-oe* and *lncRNA4-oe* plant. Bars represented standard errors (SE), * represented the significant difference ($p < 0.05$), and ** represented the highly significant difference ($p < 0.01$). Values were reported as means ± SE ($n = 4$).

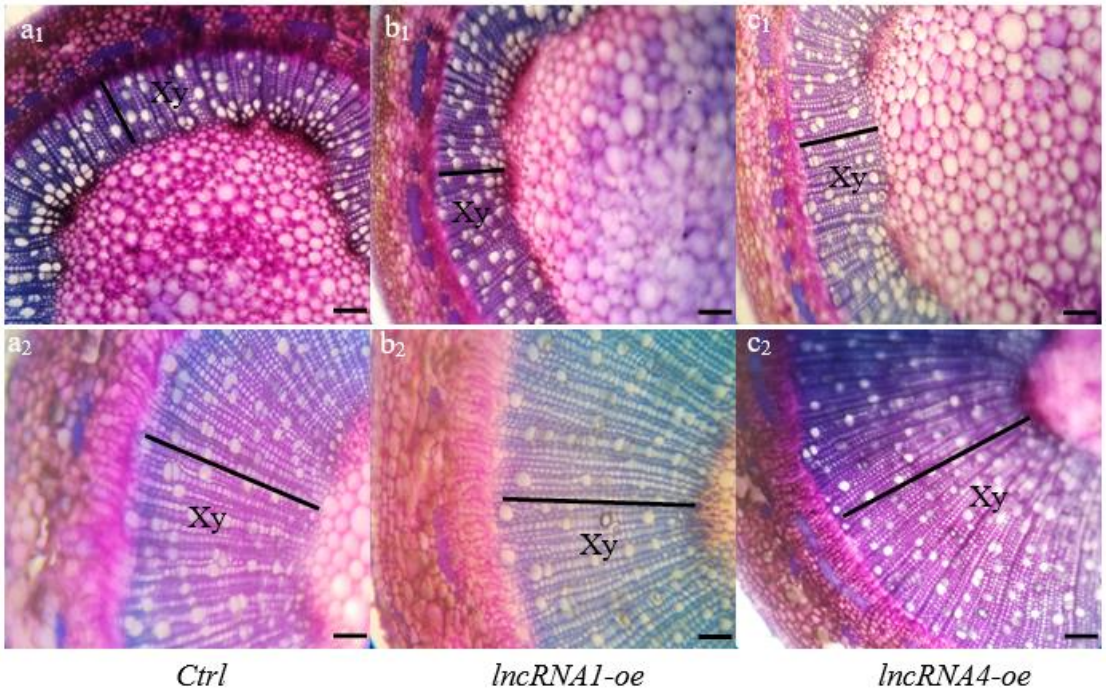

Figure 9. The slice of overexpression and wild type 84K poplar trees. (**a1**) represented the central stem, (**a2**) was the basal part of ten-week-old wild type 84K. (**b1**) represented the central stem, (**b2**) was the basal part of ten-week-old lncRNA1-oe. (**c1**) represented central stem, (**c2**) was the basal part of ten-week-old lncRNA4-oe. Xy represented xylem. Scale bar was 200 μm.

4. Discussion

The present study found 3000 new lncRNAs in each sample compared to a previous study that showed 551 new lncRNAs in the leaves and stems of *E. grandis* [19]. Annotation of lncRNA targets revealed their involvement in many physiological processes like photosynthesis, ubiquitin-mediated proteolysis, and protein output and processing from the endoplasmic reticulum. A total of 4481 intergenic lncRNAs, 761 antisense lncRNAs, and 710 intron lncRNAs were identified in different stages of development in poplar [47]. In Cassava, 833 transcripts were classified into 652 intergenic and 181 antisense lncRNAs strictly based on genomic locations [48]. This study detected 2122 intergenic lncRNAs, 239 bi-directional lncRNAs, no intron lncRNAs, and 341 antisense lncRNAs. Studies show that lncRNAs regulate gene expression in both the nucleus and cytoplasm via diversified pathways. In the nucleus, lncRNAs modulate gene expression by affecting chromatin remodeling, epigenetic modifications, and alternative splicing [49]. Our research screened four lncRNAs, viz., XR_001980078.1, XR_720796.2, XR_727233.2, and XR_001985124.1, which could be closely related to cellulose synthesis in *E. grandis*. In *P. tomentosa*, 1377 lncRNAs were identified in the xylem of tension wood, contrast wood, and normal wood, and 15,691 lncRNAs were identified in the vascular cambium, developed xylem and mature xylem. Both UGTRL and NERDL might be involved in wood formation through regulation [16,17]. In *E. grandis*, lncRNA might act as a potential target or mimic to interact with miRNA, consistent with poplar lncRNA's interaction [47]. In this study, two lncRNAs related to cellulose synthesis of *E. grandis* were cloned, and vectors were constructed. Further experiments will be carried out about genetic transformation to verify its function.

In this study, five miRNAs, viz., mir5298-y, mir3951-x, mir5198-y, mir5156-x, and mir5298-y, were closely related to cellulose synthesis of *E. grandis*. Mcnair [50] found expression patterns of 12 miRNAs in typical and fast-growing Eucalyptus trees. Pappas et al. [27] used high-throughput sequencing to excavate the xylem of two *E. globulus* genotypes, and obtained significant miRNA information. Lin et al. [51] showed that 41 miRNAs were associated with the wood formation of *E. grandis*, mainly regulating transcription factors. Although many miRNAs have been identified in plants, their functions are still not fully elucidated. Future studies should explore the combined functions of miRNA and its regulatory mechanism. Furthermore, the regulatory roles of miRNAs and their interrelationships and regulatory networks should be clarified to use these miRNAs better and apply them to crop breeding and production practice through corresponding biotechnological means.

The circRNAs found in this study were mainly antisense and exon-intron; intronic circRNAs had the least number. However, CircRNAs not only originate from exons (such as exon-derived circRNAs), introns (such as intron circRNAs), and intergenic regions [30,52,53], but some are derived from exon-intron origin RNA, exon-intron circRNA, EIciRNA [12,54,55], and even from introns of transport RNA (such as tricRNA) [48].

This study selected ceRNA and mRNA related to cellulose synthesis to construct co-expression regulatory networks, with miRNA as the center, connecting different lncRNAs, mRNAs, and circRNAs. CircRNAs have been found to function primarily as miRNA sponges. CDR1as, also known as cIRS-7, has been found to contain more than 70 conserved miR7-binding sites. Due to the binding of ciRS-7 with miR7, the expression levels of the miR7 target gene significantly increased due to decreased activity. Once the cyclic NRAciRS-7 was degraded, miR7 was released [56].

Furthermore, circRNAs positively regulated Pol II transcription by interacting with Pol II [55]. Studies have shown that EIciRNAs could micro-regulate the expression of parent genes by interacting with U1 snRNA. This discovery revealed the role of circRNAs in transcriptional regulation and the regulatory mechanism of specific interaction between EIciRNA and U1 snRNA [57]. In summary, the interaction of circRNAs with transcription mechanisms provides new insights into the regulatory mechanisms of gene expression in cells and ceRNA network mechanisms.

In this study, *lncRNA1* and *lncRNA4* were overexpressed in poplar. Moreover, cellulose and lignin contents in *lncRNA4-oe* at three weeks of seedling age were significantly higher than those in *lncRNA1-oe* and wild-type 84K poplar. The hemicellulosic content of *lncRNA4-oe* was significantly higher than that of *lncRNA1-oe* and wild-type poplar 84K, indicating that the cis-acting target gene CesA7 of *lncRNA4* promoted cellulose and lignin synthesis. The average plant height, root length, and root number of *lncRNA4-oe* at three weeks of seedling age were significantly higher than wild-type poplar 84K and *lncRNA1-oe*. Similar results were obtained even at ten weeks of seedling age. The increase of xylem cells in *lncRNA4-oe* was more extensive than that in wild-type plants and *lncRNA1-oe*. The mechanism of lncRNA regulating target genes needs to be further explored.

5. Conclusions

In this study, RNA-sequence transcriptome analysis was performed on different tissues of immature xylem in the trunk to identify ceRNA (lncRNA, miRNA, circRNA) in the process of cellulose formation in *E. grandis*. As a result, four lncRNAs, viz., XR_001980078.1, XR_001985124.1, XR_727233.2 and XR_720796.2, and five miRNAs, such as miR5298-y, miR3951-x, miR5198-y, miR5156-x, and miR5298-y that could be closely related to cellulose synthesis were screened out. In addition, the ceRNA co-expression network related to cellulose synthesis of *E. grandis* was constructed, and *lncRNA4* showed potential. These results have laid a foundation for further research on the expression and regulation of genes related to cellulose synthesis in *E. grandis*.

Supplementary Materials: The following are available online at https://www.mdpi.com/article/10.3390/f12111565/s1, Figure S1: Sampling diagram of trunk parts of *E. grandis*. (1) represented the DBH, which is 1.4 m from the ground; (2) represented the middle part of the trunk, about 10.5 m from the ground. (3) represented the upper part of the trunk, which is about 21.0 m from the ground, Figure S2: Total RNA extraction from *E. grandis* immature xylem M2Kb, molecular marker2000 bp, Figure S3: Electrophoresis for PCR product of *lncRNA1* and *lncRNA4* cloning, Table S1: Primer sequence of target gene qPCR, Table S2: Primer sequence, Table S3: Primer sequences of positive control test, Table S4: Genome comparative statistics, Table S5: Statistics on the number of transcripts, Table S6: Filtering statistics of each sample data, Table S7: The tag statistics of samples, compared with the genome, Table S8: Statistics of known miRNA number and tag abundance identified in each sample, Table S9: The number of novel miRNA identified in each sample and the abundance statistics of tag, Table S10: Predictive statistics of all miRNA target gene loci, Table S11: Statistics on new predictive targeting relationships of circRNAs.

Author Contributions: Conceptualization, Y.X. and Z.W. (Zhihua Wu).; methodology, Y.X.; software, Z.W. (Zhen Wang); validation, Z.W. (Zhihua Wu) and N.Z.; formal analysis, X.S.; investigation, N.Z.; resources, Z.W. (Zhihua Wu); data curation, G.L.; writing—original draft preparation, N.Z.; writing—review and editing, N.Z.; visualization, Z.W. (Zhihua Wu); supervision, Y.X.; project administration, Z.W. (Zhihua Wu); funding acquisition, Z.W. (Zhihua Wu). All authors have read and agreed to the published version of the manuscript.

Funding: This research was funded by Central Non-Profit Research Institution of CAF, Grant number CAFYBB2017ZX001-5 and this research was financially supported by the Fundamental Research Funds for the Central Non-profit Research Institution of Chinese Academy of Forestry, Project Number CAFYBB2019MA006.

Data Availability Statement: The data presented in this study are available on request from the corresponding author.

Acknowledgments: We thank Sichuan Academy of Forestry for their administrative support and crucial help including transport and provision of knowledgeable field assistants), tree species identification.

Conflicts of Interest: The authors declare no conflict of interest.

References

1. Tredenick, E.C.; Farquhar, G.D. Dynamics of Moisture Transport in Plant Cuticles: The Role of Cellulose. *arXiv* **2021**, arXiv:2102.08666v1.
2. Plomion, C.; Leprovost, G.; Stokes, A. Wood formation in trees. *Plant Physiol.* **2015**, *127*, 1513–1523. [CrossRef]
3. Steck, E.; Boeuf, S.; Gabler, J.; Werth, N.; Schnatzer, P.; Diederichs, S.; Richter, W. Regulation of H_{19} and its encoded microRNA-6_{75} in osteoarthritis and under anabolic and catabolic in vitro conditions. *J. Mol. Med.* **2012**, *90*, 1185–1195. [CrossRef]
4. Batista, P.J.; Chang, H.Y. Long non-coding RNAs: Cellular address codes in development and disease. *Cell* **2013**, *152*, 1298–1307. [CrossRef] [PubMed]
5. Statello, L.; Guo, C.-J.; Chen, L.-L.; Huarte, M. Gene regulation by long non-coding RNAs and its biological functions. *Nat. Rev. Mol. Cell Biol.* **2021**, *22*, 96–118. [CrossRef]
6. Zhang, H.; Guo, H.; Hu, W.; Ji, W. The emerging role of long non-coding RNAs in plant defense against fungal stress. *Int. J. Mol. Sci.* **2020**, *21*, 2659. [CrossRef]
7. Wilusz, J.E. Long noncoding RNAs: Re-writing dogmas of RNA processing and stability. *Biochim. Biophys. Acta BBA-Gene Regul. Mech.* **2016**, *1859*, 128–138. [CrossRef]
8. Zhang, Y.; Tao, Y.; Liao, Q. Long noncoding RNA: A crosslink in biological regulatory network. *Brief. Bioinform.* **2017**, *19*, 930–945. [CrossRef]
9. Wang, H.; Chung, P.J.; Liu, J.; Jang, I.-C.; Kean, M.J.; Xu, J.; Chua, N.-H. Genome-wide identification of long noncoding natural antisense transcripts and their responses to light in Arabidopsis. *Genome Res.* **2014**, *24*, 444–453. [CrossRef]
10. Zhang, J.-W.; Xu, L.; Wu, Y.-R.; Chen, X.-A.; Liu, Y.; Zhu, S.-H.; Ding, W.-N.; Wu, P.; Yi, K.-K. OsGLU3, a putative membrane-bound endo-1, 4-beta-glucanase, is required for root cell elongation and division in rice (*Oryza sativa* L.). *Mol. Plant* **2012**, *5*, 176–186. [CrossRef] [PubMed]
11. Cagirici, H.B.; Alptekin, B.; Budak, H. RNA sequencing and co-expressed long non-coding RNA in modern and wild wheats. *Sci. Rep.* **2017**, *7*, 10670. [CrossRef]
12. Li, Z.; Huang, C.; Bao, C.; Chen, L.; Lin, M.; Wang, X.; Zhong, G.; Yu, B.; Hu, W.; Dai, L. Exon-intron circular RNAs regulate transcription in the nucleus. *Nat. Struct. Mol. Biol.* **2015**, *22*, 256–264. [CrossRef]
13. Lv, Y.; Liang, Z.; Ge, M.; Qi, W.; Zhang, T.; Lin, F.; Peng, Z.; Zhao, H. Genome-wide identification and functional prediction of nitrogen-responsive intergenic and intronic long non-coding RNAs in maize (*Zea mays* L.). *BMC Genom.* **2016**, *17*, 350. [CrossRef] [PubMed]
14. Lu, X.; Chen, X.; Mu, M.; Wang, J.; Wang, X.; Wang, D.; Yin, Z.; Fan, W.; Wang, S.; Guo, L. Genome-wide analysis of long noncoding RNAs and their responses to drought stress in cotton (*Gossypium hirsutum* L.). *PLoS ONE* **2016**, *11*, e0156723. [CrossRef]
15. Zhu, Y.; Chen, L.; Zhang, C.; Hao, P.; Jing, X.; Li, X. Global transcriptome analysis reveals extensive gene remodeling, alternative splicing and differential transcription profiles in non-seed vascular plant *Selaginella moellendorffii*. *BMC Genom.* **2017**, *18*, 1042. [CrossRef]
16. Zhou, D.; Du, Q.; Chen, J.; Wang, Q.; Zhang, D. Identification and allelic dissection uncover roles of lncRNAs in secondary growth of *Populus tomentosa*. *DNA Res.* **2017**, *24*, 473–486. [CrossRef]
17. Shi, W.; Quan, M.; Du, Q.; Zhang, D. The interactions between the long non-coding RNA NERDL and its target gene affect wood formation in *Populus tomentosa*. *Front. Plant Sci.* **2017**, *8*, 1035. [CrossRef] [PubMed]
18. Gao, C.; Sun, J.; Dong, Y.; Wang, C.; Xiao, S.; Mo, L.; Jiao, Z. Comparative transcriptome analysis uncovers regulatory roles of long non-coding RNAs involved in resistance to powdery mildew in melon. *BMC Genom.* **2020**, *21*, 125. [CrossRef]
19. Lin, Z.; Long, J.; Yin, Q.; Wang, B.; Li, H.; Luo, J.; Wang, H.C.; Wu, A.-M. Identification of novel lncRNAs in *Eucalyptus grandis*. *Ind. Crop. Prod.* **2019**, *129*, 309–317. [CrossRef]
20. Axtell, M.J. Classification and comparison of small RNAs from plants. *Annu. Rev. Plant Biol.* **2013**, *64*, 137–159. [CrossRef]
21. Park, S.-M.; Peter, M.E. microRNAs and death receptors. *Cytokine Growth Factor Rev.* **2008**, *19*, 303–311. [CrossRef]
22. Meng, X.; Li, A.; Yu, B.; Li, S. Interplay between miRNAs and lncRNAs: Mode of action and biological roles in plant development and stress adaptation. *Comput. Struct. Biotechnol. J.* **2021**, *19*, 2567–2574. [CrossRef]
23. Sun, X.; Wang, C.; Xiang, N.; Li, X.; Yang, S.; Du, J.; Yang, Y.; Yang, Y. Activation of secondary cell wall biosynthesis by miR319-targeted TCP 4 transcription factor. *Plant Biotechnol. J.* **2017**, *15*, 1284–1294. [CrossRef] [PubMed]
24. Reinhart, B.J.; Weinstein, E.G.; Rhoades, M.W.; Bartel, B.; Bartel, D.P. MicroRNAs in plants. *Genes Dev.* **2002**, *16*, 1616–1626. [CrossRef]
25. Mica, E.; Gianfranceschi, L.; Pe, M.E. Characterization of five microRNA families in maize. *J. Exp. Bot.* **2006**, *57*, 2601–2612. [CrossRef]
26. Wang, L.; Du, H.; Wuyun, T.-N. Genome-wide identification of microRNAs and their targets in the leaves and fruits of *Eucommia ulmoides* using high-throughput sequencing. *Front. Plant Sci.* **2016**, *7*, 1632. [CrossRef] [PubMed]
27. Pappas, M.; Reis, A.; Farinell, L.; Pasquali, G.; Pappas, G.; Grattapaglia, D. Interspecific discovery and expression profiling of *Eucalyptus micro* RNAs by deep sequencing. *BMC Proc.* **2011**, *5*, P173. [CrossRef]
28. Nigro, J.M.; Cho, K.R.; Fearon, E.R.; Kern, S.E.; Ruppert, J.M.; Oliner, J.D.; Kinzler, K.W.; Vogelstein, B. Scrambled exons. *Cell* **2016**, *64*, 607–613. [CrossRef]
29. Liu, Q.; Zhang, X.; Hu, X.; Dai, L.; Fu, X.; Zhang, J.; Ao, Y. Circular RNA related to the chondrocyte ECM regulates MMP13 expression by functioning as a MiR-136 'Sponge'in human cartilage degradation. *Sci. Rep.* **2016**, *6*, 22572. [CrossRef]

30. Chen, L.-L.; Yang, L. Regulation of circRNA biogenesis. *RNA Biol.* **2015**, *12*, 381–388. [CrossRef]
31. Andreeva, K.; Cooper, N.G. Circular RNAs: New players in gene regulation. *Adv. Biosci. Biotechnol.* **2015**, *6*, 433. [CrossRef]
32. Ye, C.-Y.; Zhang, X.; Chu, Q.; Liu, C.; Yu, Y.; Jiang, W.; Zhu, Q.-H.; Fan, L.; Guo, L. Full-length sequence assembly reveals circular RNAs with diverse non-GT/AG splicing signals in rice. *RNA Biol.* **2016**, *14*, 1055–1063. [CrossRef]
33. Darbani, B.; Noeparvar, S.; Borg, S. Identification of circular RNAs from the parental genes involved in multiple aspects of cellular metabolism in barley. *Front. Plant Sci.* **2016**, *7*, 776. [CrossRef]
34. Zuo, J.; Wang, Q.; Zhu, B.; Luo, Y.; Gao, L. Deciphering the roles of circRNAs on chilling injury in tomato. *Biochem. Biophys. Res. Commun.* **2016**, *479*, 132–138. [CrossRef]
35. Trapnell, C.; Roberts, A.; Goff, L.; Pertea, G.; Kim, D.; Kelley, D.R.; Pimentel, H.; Salzberg, S.L.; Rinn, J.L.; Pachter, L. Differential gene and transcript expression analysis of RNA-seq experiments with TopHat and Cufflinks. *Nat. Protoc.* **2012**, *7*, 562–578. [CrossRef] [PubMed]
36. Guo, J.C.; Fang, S.S.; Wu, Y.; Zhang, J.H.; Chen, Y.; Liu, J.; Wu, B.; Wu, J.R.; Li, E.M.; Xu, L.Y.; et al. CNIT: A fast and accurate web tool for identifying protein-coding and long non-coding transcripts based on intrinsic sequence composition. *Nucleic Acids Res.* **2019**, *47*, W516–W522. [CrossRef] [PubMed]
37. Robinson, M.D.; McCarthy, D.J.; Smyth, G.K. edgeR: A Bioconductor package for differential expression analysis of digital gene expression data. *Bioinformatics* **2010**, *26*, 139–140. [CrossRef] [PubMed]
38. Zhang, D.N.; Liu, Y.; Wang, Y.F. MiRdetector: A Computational Tool to Predict and Detect miRNA Genes. *J. Shanghai Univ.* **2006**, *12*, 376–382.
39. Antheia, K.; Jon, J.; Tomas, L.L.; Ab Dimajid, O. Biological coefficient of variation of samples S1, S2 and S3 as estimated by TopHat/HTSeq/edgeR software. *PLoS ONE* **2013**, *8*, e81809.
40. Chen, L.; Yu, Y.; Zhang, X.; Liu, C.; Ye, C.; Fan, L. PcircRNA_finder: A software for circRNA prediction in plants. *Bioinformatics* **2016**, *32*, 3528–3529. [CrossRef]
41. Livak, K.J.; Schmittgen, T.D. Analysis of relative gene expression data using real-time quantitative PCR and the $2^{-\Delta\Delta Ct}$ method. *Methods* **2001**, *25*, 402–408. [CrossRef] [PubMed]
42. Shannon, P. Cytoscape: A Software Environment for Integrated Models of Biomolecular Interaction Networks. *Genome Res.* **2003**, *13*, 2498–2504. [CrossRef] [PubMed]
43. Ren, L.; Zhu, B.Q.; Zhang, Y.B.; Wang, H.Y.; Ba, C.F. The research of applying primer premier 5.0 to design PCR primer. *J. Jinzhou Med Coll.* **2004**, *25*, 43–46.
44. Liu, B.; Zhang, J.; Wang, L.; Li, J.; Zheng, H.; Chen, J.; Lu, M. A survey of Populus PIN-FORMED family genes reveals their diversified expression patterns. *J. Exp. Bot.* **2014**, *65*, 2437–2448. [CrossRef] [PubMed]
45. Lu, Q.; Shao, F.; Macmillan, C.; Wilson, I.W.; Van der Merwe, K.; Hussey, S.G.; Myburg, A.A.; Dong, X.; Qiu, D. Genomewide analysis of the lateral organ boundaries domain gene family in Eucalyptus grandis reveals members that differentially impact secondary growth. *Plant Biotechnol. J.* **2018**, *16*, 124–136. [CrossRef]
46. Etchells, J.P.; Mishra, L.S.; Kumar, M.; Campbell, L.; Turner, S.R. Wood formation in trees is increased by manipulating PXY-regulated cell division. *Curr. Biol.* **2015**, *25*, 1050–1055. [CrossRef]
47. Liu, S.; Sun, Z.; Xu, M. Identification and characterization of long non-coding RNAs involved in the formation and development of poplar adventitious roots. *Ind. Crop. Prod.* **2018**, *118*, 334–346. [CrossRef]
48. Ding, Z.; Tie, W.; Fu, L.; Yan, Y.; Liu, G.; Yan, W.; Li, Y.; Wu, C.; Zhang, J.; Hu, W. Strand-specific RNA-seq based identification and functional prediction of drought-responsive lncRNAs in cassava. *BMC Genom.* **2019**, *20*, 214. [CrossRef]
49. Long, Y.; Wang, X.; Youmans, D.T.; Cech, T.R. How do lncRNAs regulate transcription? *Sci. Adv.* **2017**, *3*, eaao2110. [CrossRef]
50. McNair, G.R. Whole-Tree and Tension Wood-Associated Expression Profiles of microRNAs in Eucalyptus Trees. Ph.D. Thesis, University of Pretoria, Pretoria, South Africa, 2009.
51. Lin, Z.; Li, Q.; Yin, Q.; Wang, J.; Zhang, B.; Gan, S.; Wu, A.-M. Identification of novel miRNAs and their target genes in Eucalyptus grandis. *Tree Genet. Genomes* **2018**, *14*, 60. [CrossRef]
52. Zhang, Y.; Zhang, X.-O.; Chen, T.; Xiang, J.-F.; Yin, Q.-F.; Xing, Y.-H.; Zhu, S.; Yang, L.; Chen, L.-L. Circular intronic long noncoding RNAs. *Mol. Cell* **2013**, *51*, 792–806. [CrossRef]
53. Suzuki, H.; Tsukahara, T. A view of pre-mRNA splicing from RNase R resistant RNAs. *Int. J. Mol. Sci.* **2014**, *15*, 9331–9342. [CrossRef]
54. Jeck, W.R.; Sorrentino, J.A.; Wang, K.; Slevin, M.K.; Burd, C.E.; Liu, J.; Marzluff, W.F.; Sharpless, N.E. Circular RNAs are abundant, conserved, and associated with ALU repeats. *RNA* **2013**, *19*, 141–157. [CrossRef] [PubMed]
55. Talhouarne, G.J.; Gall, J.G. Lariat intronic RNAs in the cytoplasm of Xenopus tropicalis oocytes. *RNA* **2014**, *20*, 1476–1487. [CrossRef]
56. Zou, Y.; Zheng, S.; Deng, X.; Yang, A.; Xie, X.; Tang, H.; Xie, X. The role of circular RNA CDR1as/ciRS-7 in regulating tumor microenvironment: A pan-cancer analysis. *Biomolecules* **2019**, *9*, 429. [CrossRef] [PubMed]
57. Lu, Z.; Filonov, G.S.; Noto, J.J.; Schmidt, C.A.; Hatkevich, T.L.; Wen, Y.; Jaffrey, S.R.; Matera, A.G. Metazoan tRNA introns generate stable circular RNAs in vivo. *RNA* **2015**, *21*, 1554–1565. [CrossRef] [PubMed]